

Predicting peak particle velocity by artificial neural networks and multivariate regression analysis - Sarcheshmeh copper mine, Kerman, Iran

H. Bakhshandeh Amnieh^{1*}, A. Mohammadi¹, M. Mozdianfard²

1. Department of Mining Engineering, University of Kashan, Kashan, Iran

2. Department of Chemical Engineering, University of Kashan, Kashan, Iran

Received 07 February 2013; received in revised form 10 May 2013; accepted 26 December 2013

*Corresponding author: bakhshandeh@kashanu.ac.ir (H. Bakhshandeh Amnieh).

Abstract

Ground vibrations caused by blasting are undesirable consequences in the mining industry and can cause serious damage to the nearby buildings and facilities. Hence, such vibrations have to be controlled to reduce the damage to the environment and this may be achieved once blasting peak particle velocity (PPV) is predicted. In this study, PPV is predicted and compared in a case study in Kerman using three methods of artificial neural network (ANN), multivariate regression analysis (MVRA) and empirical relations. The data gathered belonged to 11 blast operations in Sarcheshmeh copper mine, Kerman. The neural network input parameters include: distance from blast point, maximum charge weight per delay, spacing, stemming and the number of drill-hole rows in each blasting operation. The network is of the multi-layer perception (MLP) type, with 24 sets of training data including 2 hidden layers, 1 output layer with the network architecture being {5-11-12-1}, and Sigmoid tangent and linear transfer functions. To ensure adequate training accuracy, the network was tested by 6 data sets; the determination coefficient and the average relative error were found to be 0.977 and 8.85% respectively, indicating the MLP network's high capability and precision in estimating the PPV. Comparison of the predicted PPV's with those obtained from MVRA and the empirical relations revealed low capabilities of these two in estimating the PPV parameter.

Keywords: Peak particle velocity, Artificial neural networks, Multivariate regression analysis, Blast operations.

1. Introduction

Blast operations for excavating open pits and underground spaces are commonly employed in industrial applications primarily due to their low cost and simplicity. The energy released after a blast, not only crushes the rock mass, but also induces vibrations in the vicinity of the blast area, which in the case of exceeding the corresponding standards it can lead to adverse side effects on the safety of the residential housings, damage to infrastructure and negative environmental impacts.

Energy waves formed inside the rock mass propagate and vibrate particles constituting the perimeter of the blast hole. Many studies have indicated particle velocity to be the appropriate parameter for measuring the induced strains [1].

Parameters that affect blast operation results may be classified into two general groups: uncontrollable parameters (e.g. geological characteristics of local surrounding and location of existing structures) and controllable ones (burden, spacing, sub-drilling, stemming, delay time, charge type and its weight per delay and blast direction) [2-4]. The first monitoring on a blast phenomenon was carried out in 1942 by Nitronobel Company [5]. Blair (1954) and Duvall and Petkof (1958) studied the relationship between vibrations, charge weight and the distance from blast point. Hagan and Kennedy (1978) and Matheu (1984) worked on the effects of charge type. Jimeno (1995) and Blair and Jiang (1995) studied the effect of charge length, and

later Singh and Vogt (1998) investigated effects of blast direction [4, 6-10].

Other researchers tried to predict the intensity of vibration by proposing different mathematical models based on the elements affecting it. They have proposed their models for a specified mine, a physical location. For instance, Konya and Walter (1990) presented a model for hard rock masses. Roy (1998) worked extensively on open pits and underground mines [11, 12]. Others such as Djordjevic (1997) have focused their researches on decreasing the intensity of vibration [13].

U.S. Bureau of Mines (USBM) (1959), Langefors and Kihlstrom (1963), Ambraseys and Hendron (1968) and Just and Free (1998) have also carried out extensive research on the PPV caused by blasts [5, 14]. Wetherelt and Hunt (2003), presented useful relationships for peak particles velocity in south Florida quarries [15]. Xu et al. (2005) and Khandelwal and Singh (2006) investigated factors affecting ground vibration in open pit mines, and using artificial neural networks (ANNs) developed a model for the ground vibration [16, 17]. In terms of utilizing ANNs, Khandelwal and Singh (2007) considered the distance from the blast face to the monitoring point, as well as the explosive charge per delay, to estimate PPV, which proved to have more accurate results than empirical relation [18]. Mohamed (2009) and Monjezi et al. (2010) used various types of neural networks to estimate PPV [19, 20]. Bakhshandeh Amnieh et al. (2010) predicted the PPV using multi-layer feed forward network in Sarcheshmeh copper mine, Kerman [21]. Other works on this includes Khandelwal and Singh (2009) and Monjezi et al. (2011) who predicted PPV using ANNs, multivariate regression analysis (MVRA) and empirical relations. Results compared with two other models, indicated high capability of artificial neural networks [22, 23]. Several studies including Khandelwal et al. (2010), Khandelwal (2011) and Mohammadnjad et al. (2012) estimated PPV using support vector machine (SVM) and compared their results with empirical relations [24-26].

In this research, vibrations in Sarcheshmeh copper mine, caused by 11 blast operations were recorded using 6 to 8 seismographs under different conditions. These recordings were prepared by PDAS 100 seismograph and several L-4C 3-component seismometers. The latter was installed in three directions; namely radial (along the blast direction with respect to the seismometer position), tangential (perpendicular to the blast

direction) and vertical. The data were then analyzed and processed by DADISP software.

2. Geological and geographical positions of Sarcheshmeh copper mine

This mine is located 160 km south-west of Kerman and 50 km from the city of Rafsanjan. Geologically, it lies in the south-eastern part of central Iran tectonomagmatic belt in Pariz tectosedimentary portion of the Dehaj-Sardoieh belt in the province of Kerman, Iran. Sarcheshmeh deposit lies approximately in the center of a zone consisting of tectonic and sedimentary materials with a general direction of northwest-southeast, from the south of Turkey to Baluchistan [27]. Figure 1 shows the copper mine location and its access roads.

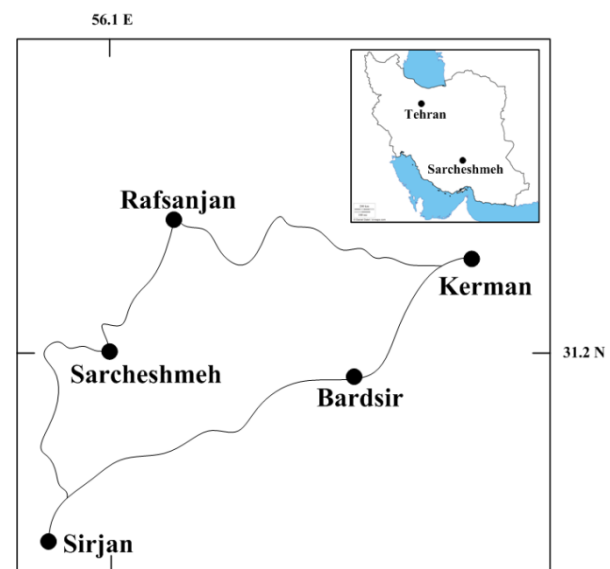


Figure 1. Schematic map of Sarcheshmeh copper mine and its access roads [27].

The mine deposit is estimated at 1.2 billion tons, being extracted using open pit method for more than 4 decades. Drilling has been carried out using machines of 200, 229 and 250mm diameter. Blast-holes patterns were mostly lozenges and considering the rock type, they were prepared with different dimensions: 8.5×6.5m for hard rocks, 9.5×7.5m for medium hard and 9.0×7.0m for soft rocks. Bench heights were about 12.5m with over-drilling of 3m, making the overall drill-hole length of approximately 15.5m. For the recorded blasts, main explosives were ANFO, Emolan and detonating cord having delays of generally 9, 17, 25, 35 and 65 milliseconds. Blasting system operated with detonating cord and non-electrical. Most recorded explosions took place in lodestone blocks, although dyke veins were also present in them [27].

3. Artificial neural network (ANN)

Inspired by the function of human brain, works on ANN started when scientists realized that human brain worked on a totally differently basis compared to common digital computers. Brain is a highly complicated processing system, made from structural units called neurons [28, 29]. ANN has been widely used in such different engineering branches as geo-technique, structure and tunneling, as well as medical sciences and management [30-33]. ANN cannot be compared to the natural nervous system as the latter becomes distinct in such applications as the separation of patterns and learning with a linear or nonlinear mapping. Such characteristics as learning potential and comparability to the existing data, extendibility, parallel processing of the network inputs (which increases the processing speed) and high error tolerability are peculiar to the neural networks [34]. ANN structure is introduced by the relation patterns among the neurons, method of finding the relation weights, and the transfer function [35]. Neural networks are usually organized by three layers. The first - the input layer - receives sources from outside of the system, the second, - the hidden layer - lies between input and output layers and is merely an intermediate result in the process of calculating the output, and the third - the output layer - is similar to the dependent variables in regression models.

Figure 2 below shows a model of a neural cell, the body of which consists of two parts: combination and transfer functions. The first combines all the inputs and produces one digit. According to Figure 2, every input has its own specific weight. The inputs are multiplied by their own related weights and then added up together to make a weighted sum which is the most common

combination function. The second part changes the value of the combination function to the cell output and then transfers it. The most common transfer function has been based upon biologic models [36].

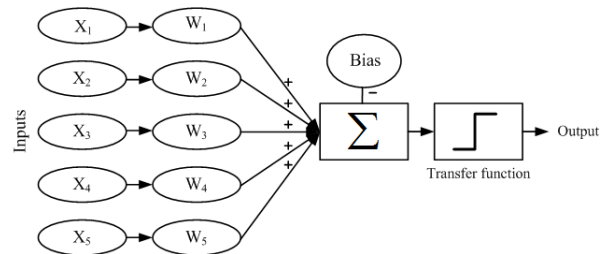


Figure 2. A simple model of a neural cell [36].

3.1. Back propagation algorithm

Back propagation algorithm (BPA) is a systematic method of training the multi-layer perception neural network (MLPNN) [37]. By training a selected network, adjusting weights and primary constants are meant in such a way that the error between the calculated and the observed output values is minimized. This algorithm is based on the error correcting learning rule. In order for the BPA to train a multi-layer feed-forward network to reach a specified goal, the training data must be presented with a proper structure. After training, the network performance can be commented on through simulating the actual and the predicted values [38].

3.2. Neural network architecture

24 data sets were used in order to train the neural network for PPV estimation. The network inputs included the distance from blast point, maximum charge weight per delay, spacing, stemming and the number of drill-hole rows in each blast, while the output is the PPV. Variation limits of input and output parameters are shown in Table 1.

Table 1. Variation limits of the input and the output parameters

Type of data	Parameter	Symbol	Range
Inputs	Distance from blast point (m)	<i>R</i>	800-2350
	Maximum charge per delay (kg)	<i>Q_{max}</i>	1620-7111
	Spacing (m)	<i>S</i>	7-9.5
	Stemming (m)	<i>T</i>	6-7
	Number of hole-rows	<i>N</i>	4-7
Output	Peak particle velocity (mm/s)	<i>PPV</i>	0.83-10.65

An effective method for training the neural networks employed commonly elsewhere is the Levenberg-Marquardt algorithm which has also been used in this research to train the network [39]. This is a back propagation algorithm

different from that of Gauss-Newton optimization method. The new weights order in the epoch (*k*+1) is calculated in the form of Equation 1:

$$w(k+1) = w(k) - (J^T J + \lambda \cdot I)^{-1} J^T \cdot \varepsilon(k) \quad (1)$$

Where J corresponds to the Jacob's matrix written for each neuron as follows:

$$J = \begin{bmatrix} \frac{\partial \varepsilon_1}{\partial w_1} & \dots & \frac{\partial \varepsilon_1}{\partial w_n} & \frac{\partial \varepsilon_1}{\partial w_0} \\ \vdots & \dots & \vdots & \vdots \\ \frac{\partial \varepsilon_p}{\partial w_1} & \dots & \frac{\partial \varepsilon_p}{\partial w_n} & \frac{\partial \varepsilon_p}{\partial w_0} \end{bmatrix} = \begin{bmatrix} x_{1_1} & \dots & x_{n_1} & 1 \\ \vdots & \dots & \vdots & \vdots \\ x_{p_1} & \dots & x_{n_p} & 1 \end{bmatrix} \quad (2)$$

where w is the weight vector, w_0 is the neuron bias, ε is the error vector (the difference between the actual and the predicted outputs) and λ is modified based on the error function of the training network. The error function for the training network is defined in the form of summing the squared error vectors. If, in each epoch, the network error is reduced, it will be acceptable, otherwise λ will vary and the new weight is re-calculated [40].

The transfer functions used in the network's hidden and output layers are of Sigmoid tangent and linear types respectively. Sigmoid is considered as the highest used transfer function; it varies slowly between the linear and nonlinear behaviors and is capable of scaling the network in the range of [-1,1]. The Sigmoid tangent transfer function is defined in the form of Equation 3:

$$f(x) = \frac{2}{1 + e^{-2x}} - 1 \quad (3)$$

Where x is the input to the function and the neuron [41].

After the transfer functions are specified in the network as being trained, use is made of an operational function called the "mean squared error" to compare the actual and the network output data. This function controls the network training through error calculation at the end of each epoch. Error estimation and duration are two important elements in the network training. BPA does not always converge to an absolute minimum; it might stop at a local minimum [42]. As shown in Figure 3, the network has a mean squared error of 1.23×10^{-29} at epoch 302.

Finally, to insure training accuracy, 6 data sets were selected randomly for the network to be tested. Using Equation 4, relative errors between actual and predicted data (shown in Table 2) were estimated. Specifications of a neural network model are briefly given in Table 3.

$$Relative\ error = \frac{PPV_{actual} - PPV_{predicted}}{PPV_{actual}} \quad (4)$$

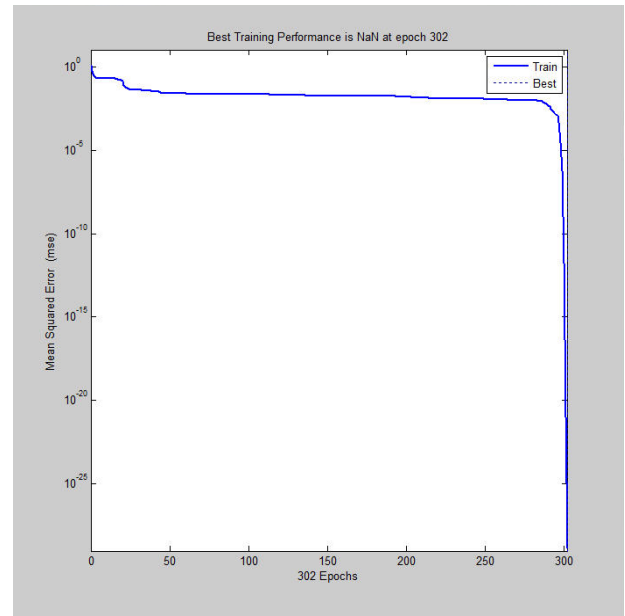


Figure 3. Mean squared error versus network epochs

Table 2. A comparison of the actual and the ANN predicted PPV

No	Actual Data	ANN predict	Relative error
1	10.01	8.8731	0.1135
2	2.33	2.1743	0.0668
3	1.22	1.2647	-0.0367
4	8.32	7.9054	0.0498
5	2.9	2.4449	0.1569
6	5.52	6.1122	-0.1072

4. Multivariate regression analysis

To find the PPV values, Equation 5 was found by applying multivariate regression analysis (MVRA) on 24 sets of data recorded from the blasts in the copper mine.

$$PPV = 13.243 - 0.00559[R] - 1.432 \times 10^{-4}[Q_{max}] + 0.159[S] + 0.289[T] - 0.422[N] \quad (5)$$

Where PPV is the peak particle velocity, (mm/s), R is Distance from blast point, (m), Q_{max} is Maximum charge weight per delay (kg), S is Spacing (m), T is Stemming (m), and N is number of drill-hole rows in each blasting operation.

Table 3. Specifications of the neural network model

Parameter	Explanation	Parameter	Explanation
No. of training data	24	Intermediate transfer function	Sigmoid Tangent (tansig)
No. of test data	6	Output layer transfer function	Linear (purelin)
Network architecture	5-11-12-1	Training function	Levenberg-Marquardt (trainlm)
Determination coefficient of test data	0.977	Performance function	Mean Squared Error (MSE)

To evaluate the above relation, the determination and the average relative error of 6 data sets from the site in question were calculated and came out to be 0.887 and 0.166 respectively. This shows that there is a considerable degree of error in estimating PPV compared to that of ANN. Figure 4 shows the correlation between the actual and the predicted values.

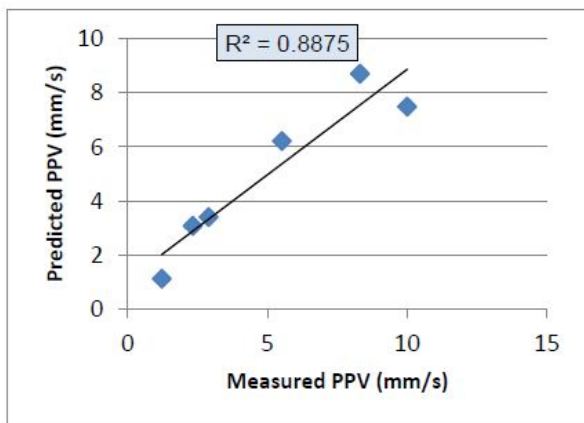


Figure 4. Predicted versus measured PPV for MVRA model (Sarcheshmeh copper mine).

5. Empirical relations for the prediction of the PPV values

As mentioned earlier, different empirical relations have been proposed so far to determine PPV values [43-48]. In these relations, intensity of vibration caused by blasting is calculated based merely on the distance from the blast point and the charge weight per delay. The general form of the relation is as follows:

$$PPV = kR^a Q_{\max}^b \quad (6)$$

Where PPV is peak particle velocity, in mm/s, R is distance from blast point, in m, Q_{\max} is maximum charge weight per delay, in kg and k , a and b is site constants. In this study, several commonly applied correlations were selected for further studies under different conditions. Site

constants were found by SPSS software using 24 sets of recorded data. Table 4 shows the results from Sarcheshmeh copper mine data analyzed with the help of 8 common empirical relations. Also, the graphs of 6 sets of seismic data, gathered from blasts and fitted on the bases of different relations, are shown in Figure 5. Considering the determination of each relation, it can be concluded that empirical relations have less capability in determining the PPV than ANN and MVRA. Amongst existing relations presented, Davies et.al and CMRI offer the least the highest average relative error, respectively.

6. Results and discussion

Figure 6 has been drawn to compare various relations and models that estimate the PPV. As shown, the values estimated by the ANN are very close to the actual values and contain less error compared with other relations. As given in Table 5, compared to other models, the highest determination coefficient and the lowest average relative error of ANN are 0.977 and 0.088 respectively.

7. Sensitivity analysis

To find how much input parameters have influenced PPV estimation, a sensitivity analysis was carried out on all 5 neural network input parameters. First, PPV values were estimated by eliminating every one of the parameters (distance from blast point, maximum charge weight per delay, spacing, stemming, and number of drill-hole rows) and reducing the input factors from 5 to 4. Then, average relative errors of the networks were evaluated for every parameter eliminated, (Figure 7). The parameter, for which the network will have the highest average relative error, can have the highest effect on the predicted PPV. As shown in Figure 7, the maximum charge weight per delay and stemming have had the most and the least effects on the PPV estimation by the ANN respectively.

Table 4. Common PPV prediction empirical relations and their results in Sarcheshmeh copper mine.

No	Name	Equation	Site Constants				
			<i>k</i>	β	α	<i>a</i>	<i>n</i>
1	USBM(1959)	$PPV = k \left[R / \sqrt{Q_{max}} \right]^{-\beta}$	113.224	1.007			
2	Langefors-Kihlstrom(1963)	$PPV = k \left[\sqrt{Q_{max} / R^{3/2}} \right]^{\beta}$	17.665	0.986			
3	Davies et al.(1964)	$PPV = kR^{-\alpha} (Q_{max})^{\beta}$	1578.554	0.179	1.012		
4	Ambraseys-Hendron(1968)	$PPV = k \left[R / (Q_{max})^{1/3} \right]^{-\beta}$	1792.470	1.314			
5	Bureau of Indian Standard(1973)	$PPV = k \left[Q_{max} / R^{2/3} \right]^{\beta}$	2.111	0.231			
6	Just-Free(1980)	$PPV = k \left[R / (Q_{max})^{1/3} \right]^{\beta} e^{-aR / (Q_{max})^{1/3}}$	8.121	0.23		0.016	
7	Ghosh-Daemen(1983)	$PPV = k \left[R / \sqrt{Q_{max}} \right]^{-\beta} e^{-aR}$	29.94	0.00001			0.001
8	CMRI (1993)	$PPV = n + k \left[R / \sqrt{Q_{max}} \right]^{-1}$	9.906				11.183

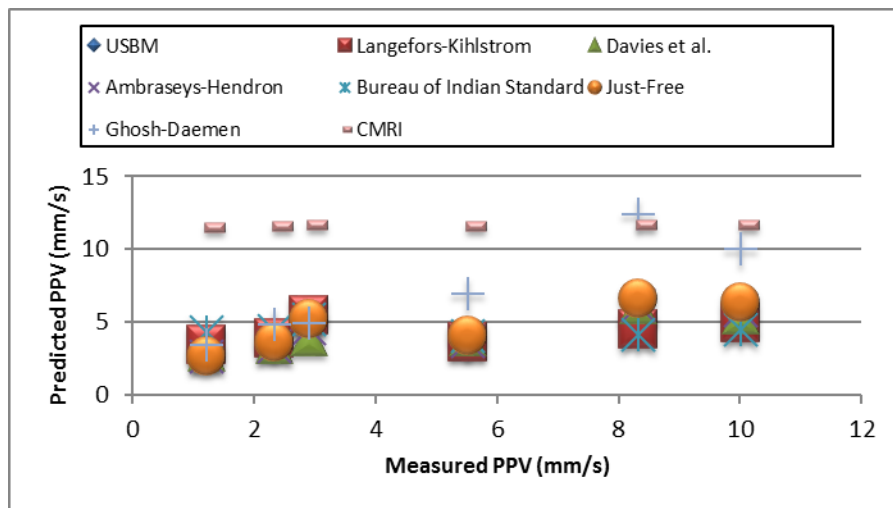


Figure 5. Predicted versus measured PPV for empirical relations values, Sarcheshmeh copper mine.

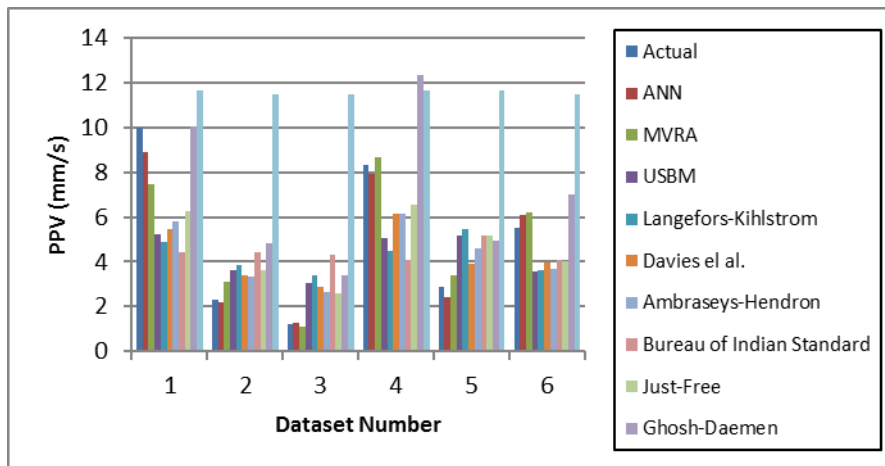
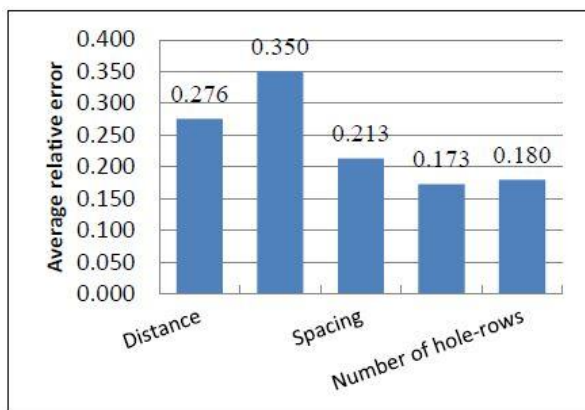


Figure 6. Comparison of the PPV results of different relations and models

Table 5. Determination coefficients and average relative error of different PPV estimation relations and models.

Model	R^2	Average relative error
ANN	0.977	0.088
MVRA	0.887	0.166
USBM	0.441	0.676
Langefors-Kihlstrom	0.134	0.776
Davies et al.	0.842	0.526
Ambraseys-Hendron	0.754	0.537
Bureau of Indian Standard	0.093	0.917
Just-Free	0.735	0.553
Ghosh-Daemen	0.866	0.716
CMRI	0.442	2.831

**Figure 7. Sensitivity analysis of the parameters affecting the estimation of the PPV**

8. Conclusions

The results, obtained by modeling using the multi-layer perception networks and 5 effective input parameters, on 30 sets of data recorded from Sarcheshmeh copper mine blasts (24 training data and 6 test data and using MATLAB) presented for training and test data of 1 and 0.977, respectively, with an average relative error of 8.85%. Therefore, considering the number of parameters and different evaluation criteria, these results may be considered as being highly precise. To estimate PPV parameters, MVRA and common empirical relations were analyzed. The results showed that these relations have weak capability for PPV estimation. ANNs have much higher capabilities for estimation of PPV compared to other models and empirical relations due to their nonlinear nature, high flexibility and low error.

References

[1]. Gustafsson, R. (1973). Swedish blasting technique: SPI Gothenburg, Sweden.

[2]. Wiss, J.F. and Linehan, P.W. (1978). Control of vibration and blast noise from surface coal mining (Vol. 103): US Bureau of Mines Report OFR.

[3]. Vogt, W. (1993). Aßbrock, Digital image processing as an instrument to evaluate rock fragmentation by blasting in open pit mines, 4th Int. in Symp. Rock fragmentation by Blasting, Keystone, Vienna, Austria. 317-324.

[4]. Jimeno, C.L., Jimeno, E.L., and Carcedo, F.J.A. (1995). Drilling and blasting of rocks.

[5]. Langefors, U. and Kihlström, B. (1963). The modern technique of rock blasting: Wiley New York.

[6]. Blair, B.E. and Duvall, W.I. (1954). Evaluation of gages for measuring displacement, velocity, and acceleration of seismic pulses: Bureau of Mines.

[7]. Duvall, W.I. and Petkof, B. (1958). Spherical propagation of explosion-generated strain pulses in rock. In: Bureau of Mines.

[8]. Hagan, T. and Kennedy, B. (1978). Practical approach to the reduction of blasting nuisances from surface operations: Aust Min, V69, N11, Nov 1977, P36-46. in International Journal of Rock Mechanics and Mining Sciences & Geomechanics Abstracts. Elsevier, 65.

[9]. Blair, D. and Jiang, J. (1995). Surface vibrations due to a vertical column of explosive. in International Journal of Rock Mechanics and Mining Sciences and Geomechanics Abstracts. Elsevier, 392A-392A.

[10]. Singh, P.K., Vogt, W., and Singh, D.P. (1998). Effect of direction of initiation on ground vibrations. International Journal of Surface Mining, Reclamation and Environment, 12, 75-78.

[11]. Konya, C.J. and Walter, E.J. (1990). Surface mine design: Englewood Cliffs, NJ: Prentice-Hall.

[12]. Roy, P.P. (1998). Technical Note Characteristics of ground vibrations and structural response to surface and underground blasting. Geotechnical and geological engineering, 16, 151-166.

[13]. Djordjevic, N. (1997). Minimizing the environmental impact of blast vibrations. Mining Engineering, 49, 57-61.

[14]. Ambraseys, N.N. and Hendron, A. (1968). Dynamic behaviour of rock masses: J. Wiley & Sons.

[15]. Wetherelt, A. and Hunt, P. (2003). Peak particle velocity modelling. in Proceeding of EFEE Second World Conference on Explosives and Blasting Technique. Prague.

[16]. Xu, Q., Wang, Q., Ji, M., Xia, W., and Sheng, W. (2005). Ground vibration model testing of bench blasting and BP neural network analysis. in Rock Fragmentation by Blasting. 591-595.

[17]. Khandelwal, M. and Singh, T. (2006). Prediction of blast induced ground vibrations and frequency in opencast mine: A neural network approach. Journal of sound and vibration, 289, 711-725.

[18]. Khandelwal, M. and Singh, T. (2007). Evaluation of blast-induced ground vibration predictors. Soil Dynamics and Earthquake Engineering, 27, 116-125.

[19]. Mohamed, M.T. (2009). Artificial neural network for prediction and control of blasting vibrations in Assiut (Egypt) limestone quarry. International Journal of Rock Mechanics and Mining Sciences, 46, 426-431.

[20]. Monjezi, M., Ahmadi, M., Sheikhan, M., Bahrami, A., and Salimi, A. (2010). Predicting blast-

induced ground vibration using various types of neural networks. *Soil Dynamics and Earthquake Engineering*, 30, 1233-1236.

[21]. Bakhshandeh Amnieh, H., Mozdianfard, M., and Siamaki, A. (2010). Predicting of blasting vibrations in Sarcheshmeh copper mine by neural network. *Safety Science*, 48, 319-325.

[22]. Khandelwal, M. and Singh, T. (2009). Prediction of blast-induced ground vibration using artificial neural network. *International Journal of Rock Mechanics and Mining Sciences*, 46, 1214-1222.

[23]. Monjezi, M., Ghafurikalajahi, M., and Bahrami, A. (2011). Prediction of blast-induced ground vibration using artificial neural networks. *Tunnelling and Underground Space Technology*, 26, 46-50.

[24]. Khandelwal, M., Kankar, P., and Harsha, S. (2010). Evaluation and prediction of blast induced ground vibration using support vector machine. *Mining Science and Technology (China)*, 20, 64-70.

[25]. Khandelwal, M. (2011). Blast-induced ground vibration prediction using support vector machine. *Engineering with Computers*, 27, 193-200.

[26]. Mohamadnejad, M., Gholami, R., and Ataei, M. (2012). Comparison of intelligence science techniques and empirical methods for prediction of blasting vibrations. *Tunnelling and Underground Space Technology*, 28, 238-244.

[27]. Najm, K., Javaherian, A., and Amnieh, H.B. (2002). Study of blasting vibrations in Sarcheshmeh copper mine. *Acta Seismologica Sinica*, 15, 683-690.

[28]. Hecht-Nielsen, R. (1989). Theory of the backpropagation neural network. in *Neural Networks, 1989. IJCNN., International Joint Conference on. IEEE*, 593-605.

[29]. Hykin, S. (1999). *Neural networks: A comprehensive foundation*. Prentice Hall International, Inc.

[30]. Yang, Y. and Zhang, Q. (1997). Analysis for the results of point load testing with artificial neural network. in *Proc Int Conf Compu Methods & Advances in Geomechanics*. 607-612.

[31]. Cai, J. and Zhao, J. (1997). Use of neural networks in rock tunneling. in *Proc Int Conf Compu Methods & Advances in Geomechanics*. 613-618.

[32]. Meulenkamp, F. and Grima, M.A. (1999). Application of neural networks for the prediction of the unconfined compressive strength (UCS) from Equotip hardness. *International Journal of Rock Mechanics and Mining Sciences*, 36, 29-39.

[33]. Singh, V., Singh, D., and Singh, T. (2001). Prediction of strength properties of some schistose rocks from petrographic properties using artificial neural networks. *International Journal of Rock Mechanics and Mining Sciences*, 38, 269-284.

[34]. Menhaj, M.B. (2002). *Fundamentals of Neural Networks (Second Edition ed.)*. Tehran: Amirkabir University of Technology Press.

[35]. Fletcher, P. (1991). A self-configuring network. *Connection Science*, 3, 35-60.

[36]. Berry, M.J. and Linoff, G.S. (2004). *Data mining techniques: for marketing, sales, and customer relationship management: ** Wiley Computer Publishing.

[37]. Rumelhart, D.E. and McClelland, J.L. (1986). *Parallel distributed processing: explorations in the microstructure of cognition. Volume 1. Foundations*.

[38]. Jain, L.C. and Fanelli, A.M. (2000). *Recent Advances in Neural Networks Design and Application*: CRC Press.

[39]. Hagan, M.T. and Menhaj, M.B. (1994). Training feedforward networks with the Marquardt algorithm. *Neural Networks, IEEE Transactions on*, 5, 989-993.

[40]. Dohnal, J. (2004). Using of Levenberg-Marquardt method in identification by neural network.

[41]. Hamed, K. and Hassan, A. (2000). An efficient tool for accelerating the numerical solution of the stochastic subsurface flow problem using neural networks. *Stochastic Environmental Research and Risk Assessment*, 14, 428-448.

[42]. Petr, V., Simoes, M., and Rozgonoyi, T. (2003). Future Development of Neural Network Prediction for Blasting Design Parameter of Production Blasting. *Explosive and Blasting Technique, Holmberg*, 625-630.

[43]. Duvall, W.I. and Fogelson, D.E. (1962). Review of criteria for estimating damage to residences from blasting vibrations. In: Bureau of Mines, College Park, MD (USA).

[44]. Davies, B., Farmer, I., and Attewell, P. (1964). Ground vibration from shallow sub-surface blasts. *Engineer*, 217.

[45]. Standard, B.o.I. (1973). Criteria for safety and design of structures subjected to underground blast (Vol. IS 6922:1973): ISI Bull.

[46]. Ghosh, A. and Daemen, J.J.K. (1983). A simple new blast vibration predictor (based on wave propagation laws). in *The 24th US Symposium on Rock Mechanics (USRMS)*.

[47]. Roy, P. (1993). Putting ground vibration predictions into practice. *Colliery Guardian*, 241, 63-7.

[48]. Birch, W. and Pegden, M. (2000). Improved prediction of ground vibrations from blasting at quarries. *Mining Technology*, 109, 102-106.